arXiv:astro-ph/0206026v2 4 Jun 2002

# Constraints of the Clumpyness of Dark Matter Halos Through Heating of the Disk Galaxies

Eliani Ardi[1], Toshio Tsuchiya

*Astronomisches Rechen-Institut, Mönchhofstr 12-14, D69120 Heidelberg, Germany*

eliani@ari.uni-heidelberg.de, tsuchiya@ari.uni-heidelberg.de

and

Andreas Burkert

*Max-Planck Institut für Astronomie, Heidelberg, Germany*

burkert@mpia-hd.mpg.de

## ABSTRACT

Motivated by the presence of numerous dark matter clumps in the Milky Way's halo as expected from the cold dark matter cosmological model, we conduct numerical simulations to examine the heating of the disk. We construct an initial galaxy model in equilibrium, with a stable thin disk. The disk interacts with dark matter clumps for about 5 Gyr. Three physical effects are examined : first the mass spectrum of the dark matter clumps, second the initial thickness of the galactic disk, and third the spatial distribution of the clumps. We find that the massive end of the mass spectrum determines the amount of disk heating. Thicker disks suffer less heating. There is a certain thickness at which the heating owing to the interaction with the clumps becomes saturates. We also find that the heating produced by the model which mimics the distribution found in Standard CDM cosmology is significant and too high to explain the observational constraints. On the other hand, our model that corresponds to the clump distribution in a ΛCDM cosmology produces no significant heating. This result suggests that the ΛCDM cosmology is preferable with respect to the Standard CDM cosmology in explaining the thickness of the Milky Way.

*Subject headings:* cosmology — dark matter — galaxies:kinematics and dynamics — methods: numerical

[1]Permanent Address : Department of Astronomy, Institute of Technology Bandung, Indonesia

## 1. Introduction

Hierarchical clustering governed by cold dark matter (CDM) is widely believed as a cosmological scenario which is responsible for the growth of the structures in the universe. According to the hierarchical scenario, small dark matter halos should collapse earlier, but later fall into larger structures. The process of smaller halos being assembled into a larger halo does not always destroy the smaller ones, thus hierarchical structures are seen in many objects, such as clusters of galaxies.

Recent high-resolution simulations have successfully shown that hundreds of galaxy-size DM halos survive in clusters of galaxies (Ghigna et al. 1998; Colin et al. 1999; Klypin et al. 1999a). A remarkable outcome of the high-resolution cosmological simulation in Standard CDM model by Moore et al. (1999) even shows that survival of substructures or satellites occurs not only on cluster scales, but also on galactic scales. They show that a galaxy of a similar size as the Milky Way should contain about 500 satellites, which is, however, much more than the number of the observationally identified satellites. That many satellites should survive, was confirmed also by Klypin et al. (1999b) and Ghigna et al. (2000). Klypin et al. note that the results of the Standard CDM simulation are close to those of a ΛCDM simulation with the same circular velocity function of substructures. This indicates that the prediction of the presence of many satellites is a general outcome of the hierarchical scenario and not particularly dependent on the cosmological models.

Compared with the observational results, these cosmological models yield a large number of the satellites, approximately a factor of 50 more than the number of satellites observed in the vicinity of the Milky Way.

Klypin et al. (1999b) suggest that the problem of the missing satellites could be resolved (i) by identification of some satellites with the high-velocity clouds observed in the Local Group (Blitz et al. 1999) or (ii) by considering dark satellites that failed to gather enough gas to form stars, because of expulsion of gas the supernova-driven winds or because of gas heating by the intergalactic ionizing background. The latter possibility implies that the halos of galaxies may contain substantial substructures in form of numerous invisible DM clumps.

A statistic of strong gravitational lensing is an approach to identify the dark clumps in the Milky Way. Chiba (2002) indeed finds evidence for the existence of the numerous satellites in the Milky Way.

If a great amount of the dark satellites exist within the Milky Way's halo, their interaction with the disk might cause disk heating. In their Standard CDM model, Moore et al. (1999) found that a large fraction of the substructures have very eccentric orbits, so that they could cause resonant heating of the disk, and even heating by impulsive shocking owing

to their penetration through the disk.

On the other hand, it is known that the Milky Way has a quite thin disk, whose scale height is about 200 pc. From the "thinness" Tóth and Ostriker (1992) have made an energetical analysis of the disk heating owing to accretion of matter, and derived the constrain that the Milky Way should have accumulated no more than 10 % of the disk mass within the past 5 Gyr. This estimation of the disk heating might, however, be too large because the actual interaction between the disk and satellites is more complicated. For example, a single satellite could dissolve before reaching the disk (Huang and Carlberg 1997) or the energy injected into the disk could excitate coherent warping motions rather than heat the disk (Velázquez and White 1999). For the case of the interaction of the disk with many substructures in the halo, additional detailed numerical investigations are necessary. Font et al. (2001) have studied the case of the ΛCDM cosmological model, and found that the substructures are not efficient perturbers for heating of the disk, since the masses of the clumps are lower than those of the clumps predicted in the Standard CDM model, and also because the clumps are located far away from the disk and seldom get near the disk.

The disk kinematics and dynamics is a good probe not only for examining the cosmological models, but much more generally for clarifying the halo substructure that is difficult to derive from direct observations. Therefore in this study we aim to investigate disk heating by dark matter (DM) clumps for a wide range of parameters.

Numerical experiments on the disk dynamics are not an easy task, especially when studying the vertical structure, because of the wide range of the dynamical scales among the different components in galaxies. The smallest scale is disk, with a scale height about 200 pc, while the largest scale is the dark halo extent of $\gtrsim 100$ kpc. Many numerical studies consider disks of 700 pc ($0.2\times$ the disk scale length) in thickness (Velázquez and White 1999; Font et al. 2001). The question is whether the heating rate obtained for such thick disks is the same as for thin disks like the real Galactic disk.

In this study we construct our initial galactic models following Kuijken and Dubinski (1995), which is nearly in exact equilibrium and which allows us to set up disks as thin as the real Galactic disk. Several additional observational constraints are taking into account to build the galactic models. We study three physical effects that could affect disk heating; first the mass spectrum of the DM clumps, second the initial thickness of the galactic disks, and the third the spatial distribution of the clumps.

This paper is organized as follows. In section 2 we present the galaxy model which provides a very stable thin disk comparable to the real Milky Way disk. A model of a clumpy dark matter halo is presented in section 3. Numerical simulations of the interaction

between disk and the clumps are specified in section 4. Section 5 presents the results of our numerical simulations on the disk heating by examining the effects on the mass spectrum of the clumps, the initial disk thickness, and the spatial distribution of the clumps. We summarize and discuss our results in section 6.

## 2. Galaxy Model

We use the self-consistent disk-bulge-halo galaxy model given by Kuijken and Dubinski (1995, hereafter KD). This model provides nearly exact solutions of the collisionless Boltzmann and the Poisson equations, so that one can control subtle differences in the initial conditions. This is important especially to set up very thin equilibrium disks, which is the most difficult part. Using this model we could successfully realize an equilibrium disk with realistic thickness of only 200 pc.

Here we summarize the model properties briefly. The configurations of the disk, bulge and halo are determined by their distribution functions. The bulge distribution function depends only on the relative energy $E$, while that of the halo depends also on the angular momentum about the symmetric axis, $L_z$.

The halo distribution function takes the form

$$f_{\rm halo}(E, L_z^2) = \begin{cases} [(AL_z^2 + B)\exp(-E/\sigma_0^2) + C]\,[\exp(-E/\sigma_0^2) - 1] & \text{if} E < 0, \\ 0 & \text{otherwise}, \end{cases} \tag{1}$$

The relative energy $E$ is defined so that $E = 0$ at the edge of the distribution, where $\rho = 0$. The halo distribution function has five free parameters: the potential at the center $\Psi_0$, which appears implicitly in the definition of the relative energy, the velocity scale $\sigma_0$, and three factors $A$, $B$, and $C$. The factors $A$ and $B$ control the system flattening ($q$) and the core radius ($R_c$), respectively, and all the three factors are scaled by the density scale ($\rho_1$).

The bulge distribution function takes the same form of a King model (Binney and Tremaine 1987)which is given by

$$f_{\rm bulge}(E) = \begin{cases} \rho_{\rm b}(2\pi\sigma_{\rm b}^2)^{-3/2}\exp[(\Psi_0 - \Psi_{\rm c})/\sigma_{\rm b}^2] & \{\exp[-(E - \Psi_{\rm c})/\sigma_{\rm b}^2] - 1\} \\ & \text{if } E < \Psi_{\rm c}, \\ 0 & \text{otherwise}. \end{cases} \tag{2}$$

This distribution depends on three parameters: the cutoff potential $\Psi_{\rm c}$, the center density $\rho_{\rm b}$, and the velocity dispersion $\sigma_{\rm b}$.

For halo and bulge distributions, the densities are given by analytic functions of $R$ and $\Psi$.

The disk distribution function must depend on three integrals of motion so that it can sustain a triaxial velocity ellipsoid within the disk. Since the third integral is not analytic, KD employ an approximate form of the distribution function which depends on $E$, $L_z$ and the vertical energy $E_z \equiv \Psi(R,z) - \Psi(R,0) + \frac{1}{2}v_z^2$. $E_z$ is only an approximate integral, but well conserved for stars in nearly circular orbits in a warm disk. This quantity is the only approximation in KD's model. The distribution function takes the form

$$f_{\rm disk}(E_{\rm p}, L_z, E_z) = \frac{\Omega(R_{\rm c})}{(2\pi^3)^{1/2}\kappa(R_{\rm c})} \frac{\tilde{\rho_{\rm d}}(R_{\rm c})}{\tilde{\sigma_R}^2(R_{\rm c})\tilde{\sigma}_z(R_{\rm c})} \exp\left[-\frac{E_p - E_{\rm c}(R_{\rm c})}{\tilde{\sigma}_R^2(R_{\rm c})} - \frac{E_z}{\tilde{\sigma}_z^2(R_{\rm c})}\right] \quad (3)$$

where $E_{\rm p} \equiv E - E_z$, $R_{\rm c}$ and $E_{\rm c}$ are the radius and energy of a circular orbit with angular momentum $L_z$. $\Omega$ and $\kappa$ are the circular and epicyclic frequencies at radius $R_{\rm c}$, respectively. The 'tilde' functions $\tilde{\rho_{\rm d}}$, $\tilde{\sigma}_R$, and $\tilde{\sigma}_z$ are free functions. Therefore the density and the radial velocity dispersion are conveniently selected as

$$\rho_{\rm disk}(R,z) = \frac{M_{\rm d}}{8\pi R_{\rm d}^2 z_{\rm d}} {\rm e}^{-R/R_{\rm d}} {\rm erfc}\left(\frac{r - R_{\rm out}}{\sqrt{2}\delta R_{\rm out}}\right) \exp\left[-4.6187 \frac{\Psi_z(R,z)}{\Psi_z(R,3z_{\rm d})}\right], \quad (4)$$

and

$$\tilde{\sigma}_R^2 = \sigma_R^2(0)\exp(-R/R_{\rm d}). \quad (5)$$

$\tilde{\rho_{\rm d}}$ and $\tilde{\sigma}_z$ are iteratively adjusted so that the densities on the mid-plane and at height $z = 3z_{\rm d}$ will agree with those given by eq. (4). The distribution of the disk has six free parameters: the disk mass $M_{\rm d}$, the radial scale length $R_{\rm d}$, the vertical scale height $z_{\rm d}$, the disk truncation radius $R_{\rm out}$, the truncation width $\delta R_{\rm out}$, and the central velocity dispersion of the disk $\sigma_R(0)$.

The choice of the above parameters is made to satisfy observational properties of the Milky Way (see also Tsuchiya (2002)), that is the solar radius $R_0 = 8$ kpc, the circular velocity of the disk at the solar radius $V_{\rm c} = 220$ km/s, the total surface density within 1.1 kpc of the disk plane $\Sigma_{1.1}(R_0) = 71 \pm 6 M_\odot {\rm pc}^{-2}$ (Kuijken and Gilmore 1991), the contribution of the disk material to $\Sigma_{1.1}$, $\Sigma_{\rm d}(R_0) = 48 \pm 9 M_\odot {\rm pc}^{-2}$ (Kuijken and Gilmore 1991), the total Galaxy mass within 50 kpc $M_{\rm tot}(< 50{\rm kpc}) = 5.4^{+0.2}_{-3.6} \times 10^{11} M_\odot$ (Wilkinson and Evans 1999), and the total Galaxy mass within 170 kpc $M_{\rm tot}(< 170{\rm kpc}) = 1.9^{+3.6}_{-1.7} \times 10^{12} M_\odot$ (Wilkinson and Evans 1999).

We assume that the disk mass is $M_{\rm d} = 5 \times 10^{10} M_\odot$, the disk scale length $R_{\rm d} = 3.5$ kpc, the disk scale height $z_{\rm d} = 245$ pc, and the disk truncation radius and the truncation width are $R_{\rm out} = 7R_{\rm d}$ and $\delta R = R_{\rm d}$, respectively. The bulge mass is about 15 % of that of the disk, while the tidal radius is 2.38 kpc. The contributions of the bulge and disk to the rotation

curve is shown in Fig. 1. We also examined thicker disks with $z_{\rm d} = 525$ pc and 1050 pc, as described in the next section.

For the halo, we assume $A$=0 in eq. 1, which means that the halo is nearly spherical, except for the flatness caused by the presence of the disk potential. As for the extent of the halo, we consider two different models. One has the virial radius at 262 kpc, with a dark matter mass of $8.59 \times 10^{11} M_{\odot}$. We refer to it as the *standard halo model*. The other has the virial radius at 1.35 Mpc, with a mass of $4.1 \times 10^{12} M_{\odot}$, which is called the *extended halo model*. The difference between the two models lies only in the outer part of the halos. The inner density profiles ($R \lesssim 50$ kpc) are about the same (Fig. 2 and Fig. 4), thus the rotation curves of the bulge, disk, and the halo are nearly equivalent between two models (Fig. 1 and Fig. 3). The extended halo model is introduced only to produce different clump distributions as described below.

The halo and the bulge are treated as an external force, while the distribution of the disk is realized by self-consistent particles.

Without the substructure clumps in the halo, this model is fairly stable. The net increase in the disk thickness is only due to 2-body relaxation among the disk particles, which is only $\Delta z_d \sim 150$ pc after 4.76 Gyr.

## 3. Dark Matter Clumps Model

The numerical cosmological simulations (Moore et al. 1999) have demonstrated the presence of the dark matter clumps within dark halos. We distribute the clumps in a similar way as shown in the numerical results.

The dark matter clumps are represented by rigid bodies with a Navarro, Frenk & White's density profile (Navarro et al. 1997). It provides an accurate fit to the density profiles of CDM halos:

$$\rho(r) = \frac{\rho_{\rm crit}\delta_{\rm c}}{(r/r_{\rm s})(1 + r/r_{\rm s})^2}. \tag{6}$$

Here $\rho_{\rm crit} = 3H^2/8\pi G$ is the critical density for closure of the universe, and $\delta_{\rm c}$ and $r_{\rm s}$ are the characteristic density and the scale radius of the clump. In practice, it is more convenient to use mass and concentration to characterize each clump instead of $\delta_{\rm c}$ and $r_{\rm s}$.

The mass of a dark matter clump, $M$, is related to its virial radius $r_{200}$, which is defined as the radius within which the average density equals 200 times the critical density at the

present $\rho_{\rm crit,0}$, by the relation

$$M = \frac{4\pi r_{200}^3}{3} 200 \rho_{\rm crit,0}. \tag{7}$$

Then the characteristic density $\delta_{\rm c}$ is expressed in terms of the concentration $c = r_{200}/r_s$ as

$$\delta_{\rm c} = \frac{200}{3} \frac{c^3}{\ln(1+c) - c/(1+c)}. \tag{8}$$

Each clump has two characteristic parameters, but we fix the concentration to a typical value $c = 20$. Since the interaction between the clumps and the disk is dominated by distant encounters, the adopted value for the concentration does not affect the heating process so much.

The simulations of Klypin et al. (1999b) and Ghigna et al. (2000) show that the total mass of the clumps is about one tenth of the halo mass. We therefore give the clumps 10 % of the halo mass of the standard model, which is $8.59 \times 10^{10} M_\odot$ in total. The distribution of positions and velocities of the clumps is assumed to be the same as the halo distribution function (eq.1), so that the clump distribution does not change in time. This is the most reasonable assumption which is important in order to maintain an equilibrium in the whole system. Otherwise the change in the mean potential of the halo might cause undesired change in the disk thickness. The background halo component, which is treated as an fixed external field, is reduced by 10 %.

The orbital properties of the clumps could be represented by the radii of their pericenters and apocenters. Fig. 5 shows the distribution of the pericenters and the apocenters of the clumps. The lines of the constant eccentricity, which is defined as $e \equiv (r_{\rm a} - r_{\rm p})/(r_{\rm a} + r_{\rm p})$ are superposed in the plot. The eccentricity distribution has a median at 0.6, which is in a good agreement with the Standard CDM simulations that predicts high eccentricity orbits with a median apocentric-to-pericentric distance of 6:1 (Moore et.al, 1999).

For the mass spectrum of the clumps, we examine three different possibilities. *Model 1* and *model 3* have only one single population of clumps with clump masses of $10^8 M_\odot$ and $10^9 M_\odot$, respectively. These two models are meant to be extreme cases. *Model 2* has a mass spectrum with a mass range of $10^8$ to $10^9 M_\odot$ according to the probability distribution

$$N(M)dM \propto M^{-2} dM, \tag{9}$$

following the cosmological prediction by Moore et al. (1999), Klypin et al. (1999b) and Ghigna et al. (2000). This model is considered to be the most realistic examination. In this model the masses are assigned randomly to the clumps. These three models were designed in order to examine the role of the individual mass of the clumps on the disk heating.

Two additional physical effects on disk heating are studied. One is the initial disk thickness. Thinner disks have smaller vertical velocity dispersions, they should therefore be more sensitive to disturbances from the clumps, and might experience a large thickening. Therefore we ran *models 4* and *5* which have an initial disk scale height of 525 pc and 1050 pc, respectively. Both models have the same mass spectrum as model 2.

Another influential property of the clumps on disk heating is the position of their pericenter, where the gravitational tides become the largest. The probability distribution of the pericentric radii of the DM clumps is shown in Fig. 6. The abscissa shows the pericentric radii of the clumps, and the ordinate shows the cumulative fraction of the number of clumps which have pericenters less than the value on the abscissa. About 18 % – 20 % of the clumps have pericenters within the solar radius. This is similar to the clump distribution obtained by Moore et al. (1999) in the Standard CDM cosmology.

In order to examine the effect of the position distribution of the clumps, we created *model 6*, which has the same mass spectrum as model 2, but the Milky Way has the density profile, according to the *extended halo model*. This model has two noticeable features; (i) the inner density profile is the same as the standard halo model so that all the kinematical properties of the disk are equivalent, and (ii) the tidal radius is 5 times larger than that in the standard model. We distribute the clumps in the same way as the halo particles. Thus their spatial distribution is also 5 times larger in radius than in the other models. In this model, the total clump mass is the same as before. Therefore, the mass fraction of the clumps to the whole halo is 2 %. The probability distribution of the pericenters is shown in Fig. 6. The number of clumps that have pericenters within the solar radius is about 3.5 %. This model corresponds to the clump distribution predicted from a ΛCDM cosmology, as demonstrated by Font et al. (2001).

The characteristic parameters of all models are summarized in Table 1.

## 4. Numerical Simulation

We calculate the interactions between the disk particles by using a hierarchical tree algorithm Hernquist (1987) with a tolerance parameter of $\theta_{\rm tol} = 0.7$. The time integration is made with the leap-frog method and a fixed time step of 1.75 Myr. The softening length of the disk particles is 70 pc. We use 131,072 particles in the disk. The forces from the clumps are calculated by direct summation. We have followed the evolution up to 4.76 Gyr.

The calculations are made on Pentium III – Linux workstations (800MHz). The typical calculation time is 90 seconds per time step.

## 5. Results

In this section we show the results of our numerical simulations on the disk heating. Three different physical effects are examined here: the mass spectrum of the clumps, the initial disk thickness, and the spatial distribution of the clumps.

Throughout the section, we are measuring the disk heating by the increase of the disk thickness, $\Delta z_d$, and by the change in the velocity dispersion, $\Delta\sigma_R$, $\Delta\sigma_z$. To calculate these quantities, the disk is stratified in concentric annuli, each of which containing 8192 particles. The disk thickness is evaluated simply by the mean square deviation of the $z$-coordinate of disk particles from the center of the disk plane, $z_d(R) \equiv \langle {z_d}^2 \rangle^{1/2}$, within the annuli.

Even without the clumps, the self-heating within the disk owing to two-body relaxation among the disk particles is always taking place in numerical simulations with modest number of particles. In our simulations with 131,072 particles in the disk, the increase owing to the self-heating is typically $\Delta z_d = 150$ pc, and $\Delta\sigma_z = 4$ km/s at the solar radius after 4.76 Gyr simulations. These values are reasonably small, but need to be taken into account when analyzing the results. The curves corresponding to the self-heating after 4.76 Gyr are shown as internal heating in Fig. 7 – Fig. 13 .

### 5.1. Mass Spectrum of the Clumps

The results of the disk heating obtained from the simulations of the model 1, 2, and 3 are shown in Fig. 7 and Fig. 8. The comparison between the results makes the effect of the mass spectrum of the DM clumps clearer.

The growth of the disk thickness in model 1 is $\Delta z_d \sim 615$ pc, 630 pc, and 900 pc at $R = 2$, 8, and 16 kpc, respectively, while those values in model 3 are 860 pc, 1298 pc, and 2197 pc. It is clear that the interaction of a galactic disk with a few, but massive clumps (model 3) is more effective to heat the disk than the interaction with many but less massive clumps. This result can be explained by the estimate in an impulsive approximation, which predicts that the increase in the energy of the disk is $\Delta E \propto N\ M^2$. If there is a mass spectrum, $dN(M) \propto M^{-2} dM = M^{-1} d(\log M)$, $\Delta E$ is dominated by massive clumps. The disk thickening obtained from model 2 (Fig. 7**b**) is, in fact, much closer to that in model 3. This result could be also understood by the impulsive approximation, as the energy input to the disk from the logarithmic interval in the mass spectrum is dominated by the more massive clumps; $d\Delta E \propto M d(\log M)$. Therefore the higher limit of the mass spectrum has an essential contribution on the disk heating.

A difference feature between models 2 and 3 is their dependence of the disk heating on the disk radius. For all models the outer part of the disk is heated up more than the inner part, but this gradient is the largest in the model 2. The increase of the disk thickness for $R < 13$ kpc is smaller in model 2 than in model 3, while it is opposite in the outer disk. In model 2, which imitates the results of the Standard CDM model, the disk thickness becomes 1 kpc at the solar radius after 4.76 Gyr interactions.

An alternative way to estimate the disk heating is the increase in the velocity dispersion. Fig. 8 shows the same results as Fig. 7. The existence of a few massive clumps has a large influence on the disk heating. This figure shows the increase in the radial (the left panels) and the vertical (the right panels) velocity dispersions. After 4.76 Gyr, the interaction of the disk with clumps in model 2 produces $\sigma_R = 60$ km/s and $\sigma_z = 35$ km/s. The properties of disk heating in model 2 seem to agree with those of the thick disk component at the solar radius which has $\sigma_R = 63$ km/s and $\sigma_z = 38$ km/s and a vertical scale length of 1 kpc (Freeman 1996).

It is noticeable that the initial velocity dispersion is not isotropic or $\sigma_R$ is larger compared to $\sigma_z$. After 4.76 Gyr, in the inner part of the disk ($R < 5$ kpc), there is no increase in the radial velocity dispersion while the vertical velocity dispersion increases a lot. This anisotropy in the heating is seen also in the outer part of the disk in model 2. A possible explanation is that the heating owing to the clumps is aiming at a more isotropic velocity dispersion.

### 5.2. Initial Disk Thickness

Our model 2 has an initial disk thickness comparable to the observed value in the Milky Way, which is about 250 pc. In many simulations in other works, however, the typical initial disk thickness was chosen much larger. For example, Font et al. (2001) employ the initial disk with a thickness of 700 pc. The susceptibility of the disks to the heating owing to the interaction with the DM clumps should depend on the initial disk thickness. Thicker disks are possibly less sensitive and suffer less heating. In order to clarify the difference in the disk heating according to the initial disk thickness, we carried out three investigations with the models 2, 4, and 5. These models have almost the same bulge, halo, and clump systems, but the initial disk thicknesses are 245 pc, 525 pc, and 1050 pc, respectively. The results of the disk heating are shown in Fig. 9, and Fig. 11.

After 4.76 Gyr, the disk in model 2 achieves a thickness of 1 kpc at the solar radius, thus the increase rate is about 400%. In models 4 and 6, the final disk thicknesses at the

solar radius are 1.1 kpc and 1.5 kpc, respectively. The increase rates in the thickness are thus 210% and 70%. This tendency is more pronounced in the inner regions. In the central region $R < 3$ kpc, the disk in model 5 has experienced nearly no heating. On the other hand, in the outer regions $R > 14$ kpc, the heating owing to the interaction with the clumps is so large that the difference in the initial disk thickness is negligible. This feature is more clearly seen in Fig. 10. The panels in the figure show the time variations of the disk thickness (a) at $R = 2$ kpc, (b) at the solar radii, and (c) at $R = 16$ kpc, respectively. It is natural that the outer part of the disk experiences more heating, because it is closer to the DM clumps. A common characteristic to all radii is that the difference in the initial disk thickness decreases in time. The curves in the panel (a) indicate that the heating will be saturated at the level of $z_d \sim 1.2$ kpc. In the outer parts the heating is still going on to make the disk even thicker. The growth of the velocity dispersions in the disks, which is shown in Fig. 11, also gives the same information namely that thicker disks suffer less heating.

This flaring effect, that is the increase in the disk thickness especially in the outer part, is seen in VLA observations of HI disk of galaxies NGC 100 and UGC 9242 (Bosma 1991). The interaction with the hypothetical DM clumps would be an explanation of this feature.

### 5.3. Spatial Distribution of the Clumps

In our models the clump's spatial distribution is the same as the halo distribution in order to ensure the equilibrium. This clump distribution, however, creates more clumps in the inner part of the halo than that obtained by the cosmological simulations. For example, Font et al (2001) employ a clump distribution in which only 3 % of the clumps have pericenters within the solar radius. Our model 6 is designed to remove the clumps from the inner region. This is accomplished by introducing a more extended equilibrium halo model. We distribute the same clumps as in the model 2 in the extended halo. The spatial extent of the clump distribution in this model becomes 5 times larger, and only 3.5 % of the clumps have pericenter within the solar radius (see Fig. 6).

The increase in disk thickness and velocity dispersion is shown in Fig. 12 and Fig. 13. In the model 6, the disk heating owing to the interaction with the clumps is comparable with the disk internal heating, up to the disk edge. In this case, we would need more precise simulations with larger number of particles, but it is already clear that even with the presence of the many clumps surviving in the halo, tidal disk heating is negligible and the disk remains as thin as the real Milky Way disk for about 5 Gyr. This result is in agreement with conclusion of Font et al. (2001).

## 6. Discussion and Conclusions

We have made a series of numerical simulations, examining heating of galactic disks that are embedded in a halo with many small DM clumps, as suggested by cosmological simulations. We have built up the initial galaxy model as precisely in equilibrium as possible, so that we could simulate a stable disk that is as thin as the Milky Way.

We have shown that with the mass spectrum $N(M)dM \propto M^{-2}dM$, that is consistent with cosmological simulations, the massive end of the mass spectrum determines the amount of disk heating. The number of the clumps at the massive end could be only a few, so that the massive limit of the spectrum might fluctuate among galactic halos. This fact suggests a variety of disk thickness because of the random fluctuation in the number of the most massive clumps.

As a second result, the simulations demonstrate that thicker disks suffer less heating. It is possible that a disk with 700 pc thickness shows no significant heating whereas another disk with 200 pc thickness suffers significant heating in the same circumstances. This also means that there is a critical thickness at which the heating owing to the interaction with the clumps is saturated.

Finally, we have considered the relation to cosmology. Our model 2 mimics the clump distribution found in the Standard CDM cosmology (Moore et al. 1999; Klypin et al. 1999b). The disk heating by the clumps has already been discussed by Moore et al. (1999). They argued by a simple impulsive approximation that disk heating would be too high to explain the age-temperature relation for disk stars (Wielen 1974). Our numerical simulations are supplementary to their analysis, and we confirm that the heating is significantly high. The thickness of 1 kpc at the solar radii is comparable to the present thick disk, but this heating takes place within 5 Gyr and even a young thin disk would have no chance to survive. On the other hand, our model 6 corresponds to the clump distribution of the ΛCDM cosmology, similar to the one Font et al. (2001) have studied, but more closely representing the Milky Way. As found by Font et al. (2001), this clump distribution causes no significant heating of the disk. These results suggest that the ΛCDM cosmology is preferable with respect to the Standard CDM cosmology in explaining the thickness of the Milky Way.

We thank Burkhard Fuchs and Andreas Just for their useful comments and suggestions. EA is grateful to Astronomisches Rechen-Institut (ARI), Heidelberg, in particular Rainer Spurzem, for allowing her to conduct simulations on ARI's Unix cluster. TT is indebted to Alexander von Humboldt foundation for research grant.

## REFERENCES

Binney, J., and Tremaine, S. 1987, Galaxy Dynamics, Princeton Univ. Press, Princeton

Blitz, L., Spergel, D.N., Teuben, P.J., Hartmen, D., and Butler-Burton, W. 1999, ApJ, 514, 818

Bosma, A. 1991 in Casertano, S., Sacket, P., and Briggs, F., eds, Warped Disks and Inclined Rings around Galaxies, Cambridge University Press p.181

Chiba, M. 2002, ApJ, 565, 17

Colin, P., Klypin, A.A., Kravtsov, A.V., and Khokholov, A.M. 1999, ApJ, 532, 32

Font, A., Navarro, J.F., Stadel, J., and Quinn, T. 2001, ApJ, 563, L1

Freeman, K.C. 1996, in Morrison, H.L., Sarjedini, A., eds, ASP Conf. Ser. Vol. 92, Formation of the Galactic Halo, Inside and Out. Astron. Soc. Pac., San Francisco, p.3

Ghigna, S., Moore, B., Governato, F., Lake, G., Quinn, T., and Stadel, J. 1998, MNRAS, 300, 146

Ghigna, S., Moore, B., Governato, F., Lake, G., Quinn, T., and Stadel, J. 2000, ApJ, 544, 616

Hernquist, L. 1987, ApJS, 64, 715

Hernquist, L. 1990, ApJ, 356, 359

Huang, S., and Carlberg, R.G. 1997, ApJ, 480, 503

Klypin, A., Gottöber, S., Kravtsov, A.V., and Khokholov, A.M 1999a, ApJ, 516, 530

Klypin, A., Kravtsov, A.V., Valenzuela, O., and Prada, F. 1999b, ApJ, 522, 82

Kuijken, K., and Dubinski, J. 1995, MNRAS, 277, 1341

Kuijken, K., and Gilmore, G. 1991, ApJ, 367, L3

Moore, B., Ghigna, S., Governato, F., Lake, G., Quinn, T., Stadel, J., and Tozzi, P. 1999, ApJ, 524, L19

Navarro, J.F., Frenk, C.S., and White, S.D.M. 1997, ApJ, 490, 493

Tóth, G., and Ostriker, J.P. 1992, ApJ, 389, 5

Tsuchiya, T. 2002 accepted for publication in New Astronomy

Velázquez, H., and White, S.D.M. 1999, MNRAS, 304, 254

Wielen, R. 1974, A&A, 60, 263

Wilkinson, M.I., and Evans, N.W. 1999, MNRAS, 310, 645

This preprint was prepared with the AAS LaTeX macros v5.0.

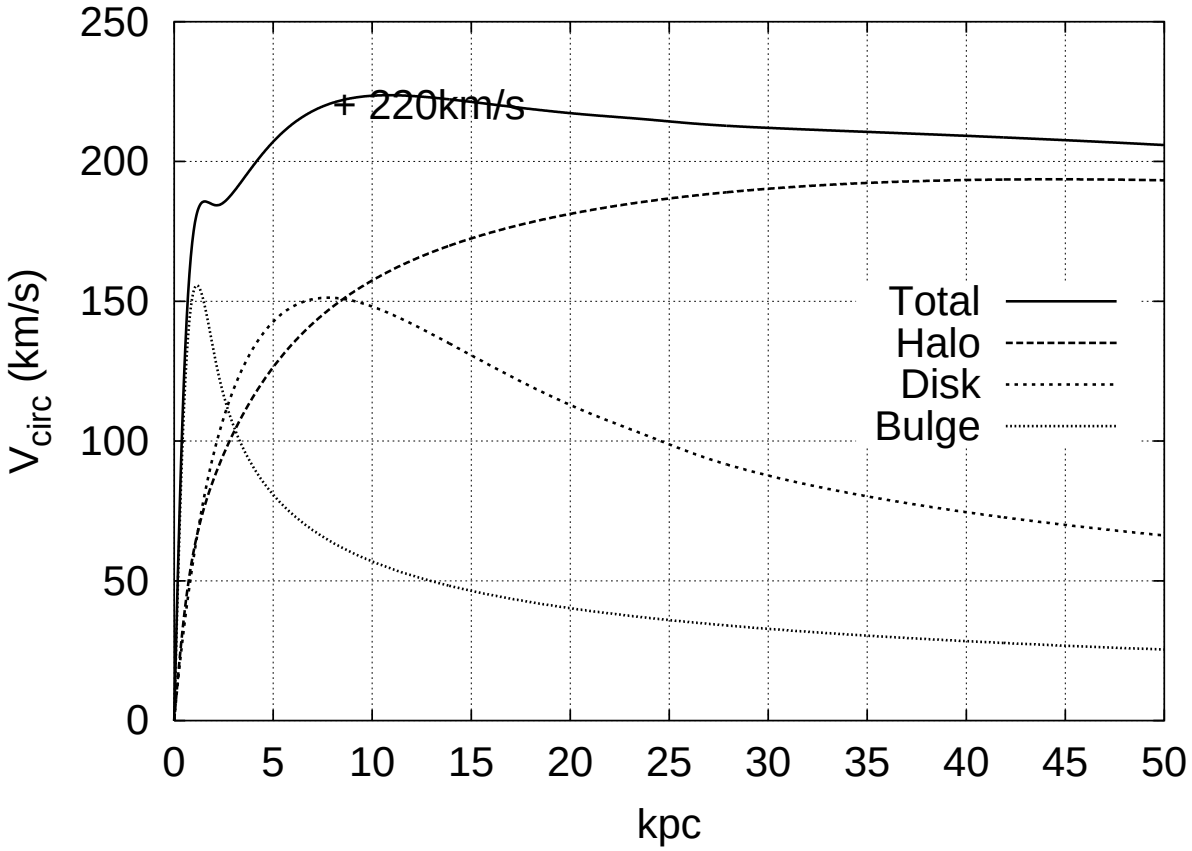


Fig. 1.— Circular velocity profiles for the Galaxy model with the standard halo. The cross sign (+) shows the observational circular velocity at the solar radius.

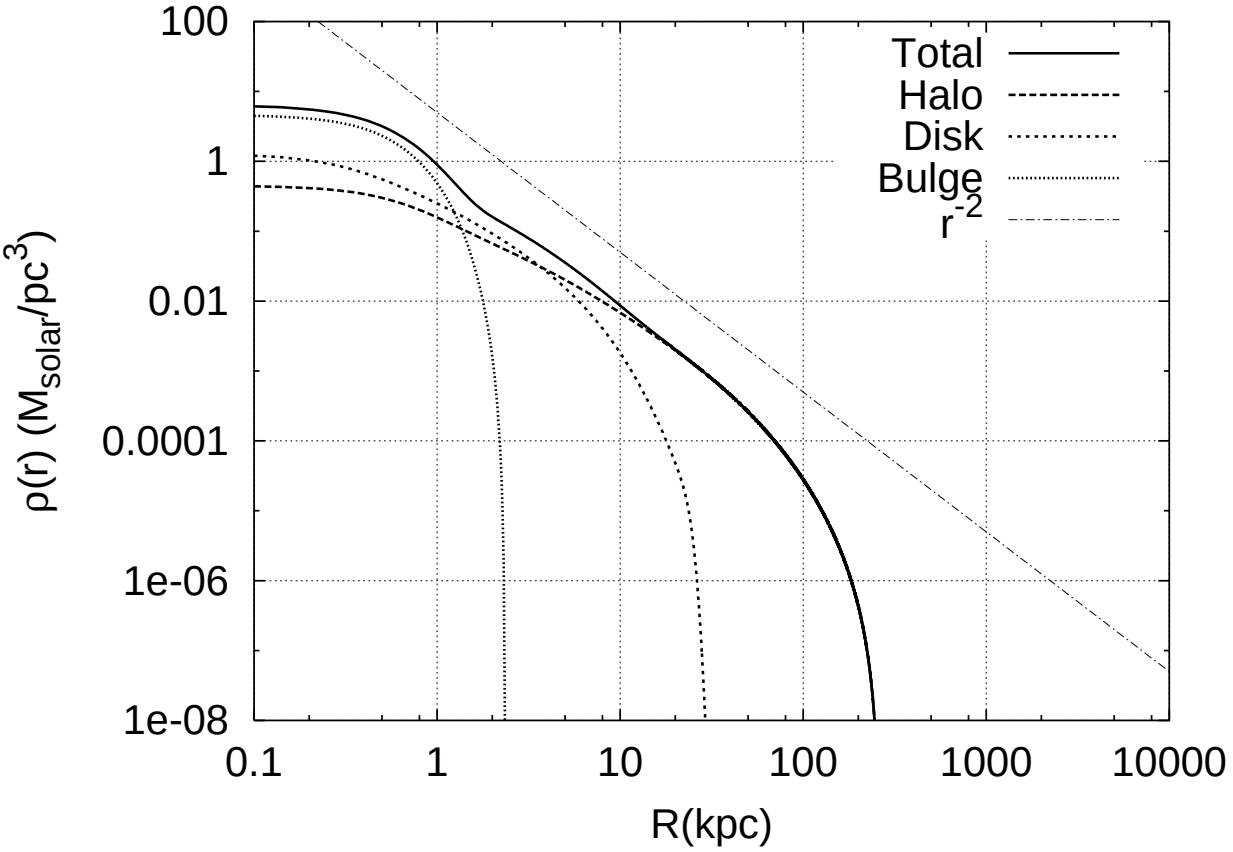


Fig. 2.— Volume density profiles of the components in the Galaxy model with the standard halo.

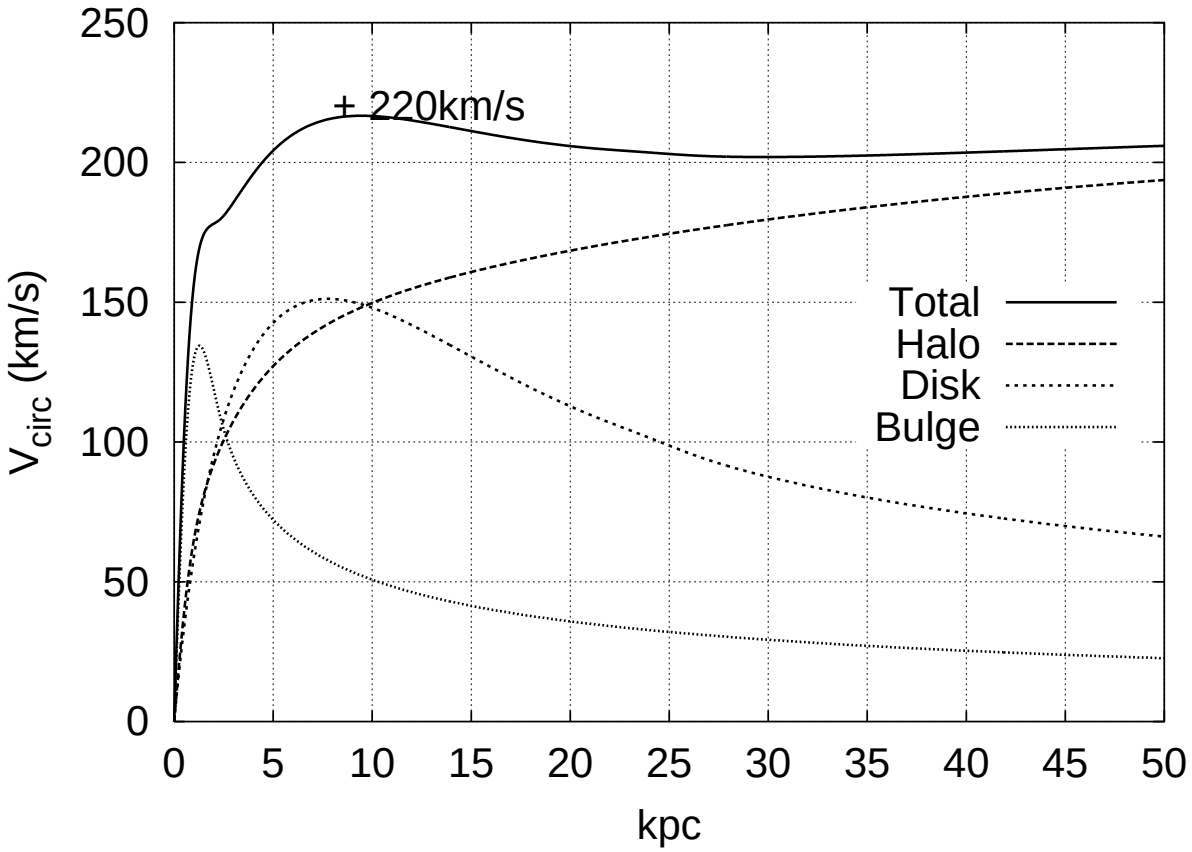


Fig. 3.— Circular velocity profiles for the extended halo model. The cross sign (+) shows the observational circular velocity at the solar radius.

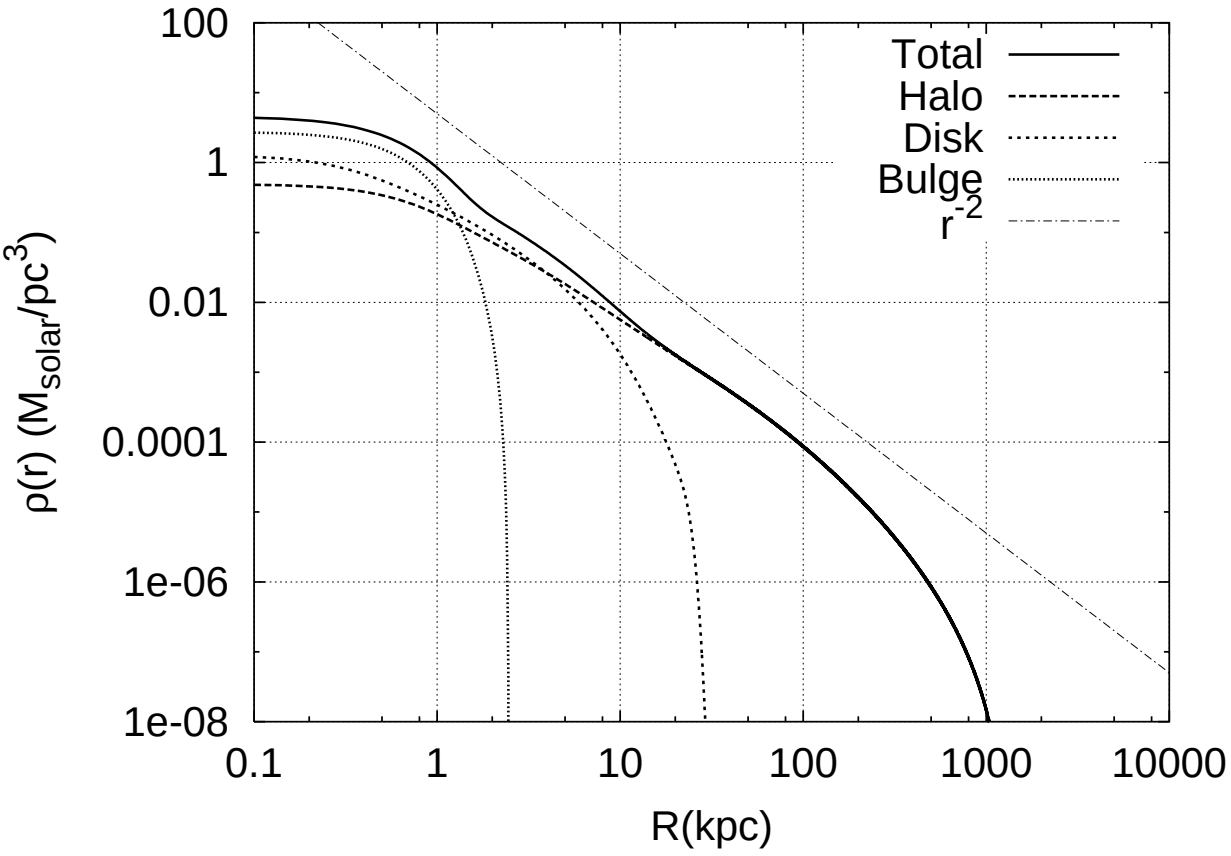


Fig. 4.— Volume density profiles of the components in the extended halo model.

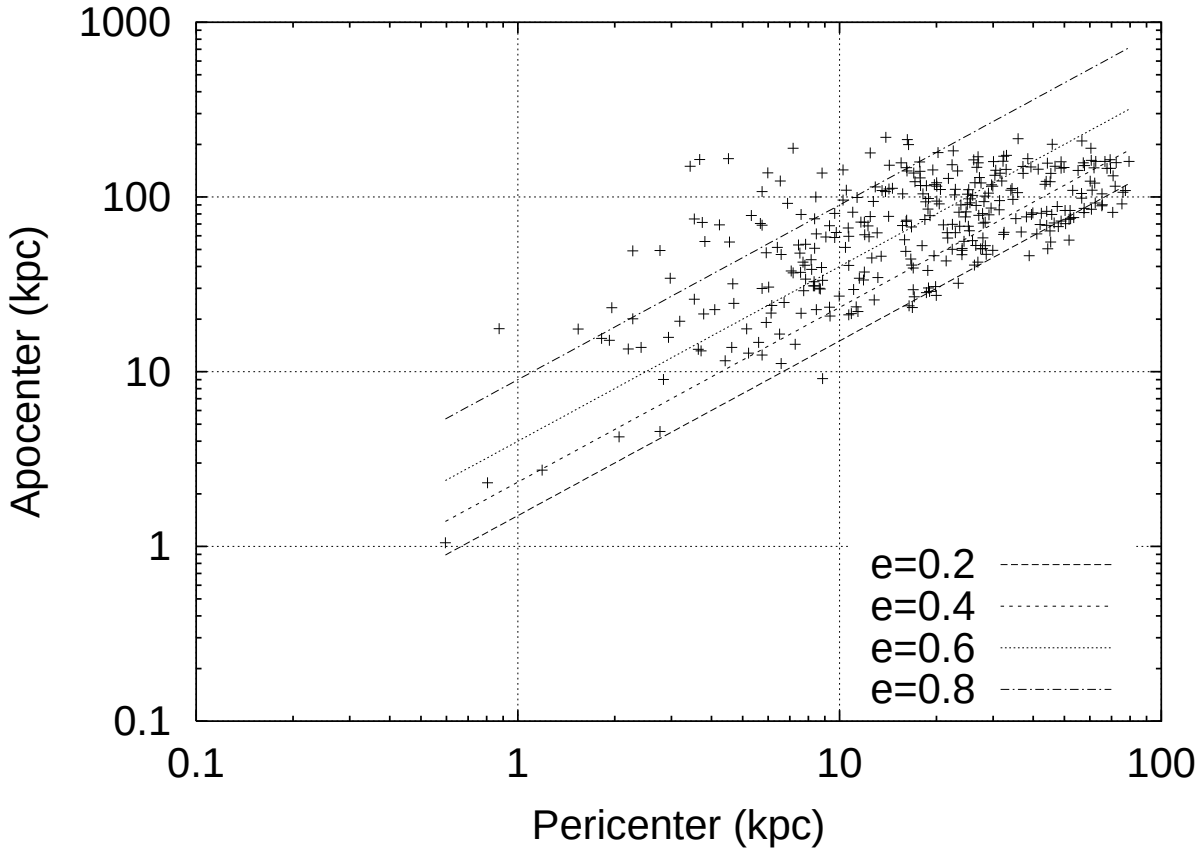


Fig. 5.— Distribution of the pericenter and the apocenter of the clumps in model 1. The cross (+) symbols indicate the individual clumps. The lines of constant eccentricity $e = 0.2$, 0.4, 0.6, and 0.8 are also shown.

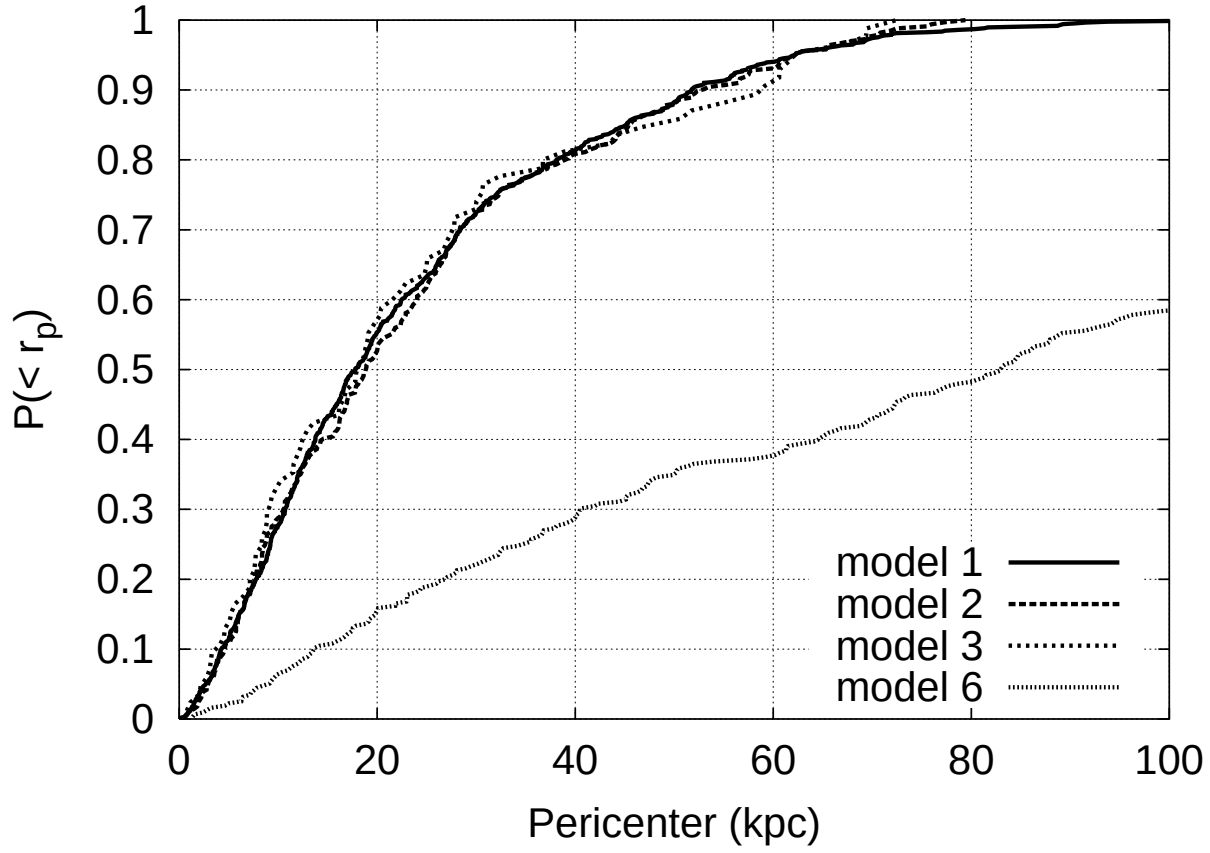


Fig. 6.— Cumulative distribution of the pericenters of the clumps in the models 1, 2, 3, and 6. The ordinate shows the fraction of the clumps which have a pericenter smaller than the value on the abscissa. In the models 1 to 3, 20 % of the clumps have pericenters smaller than 10 kpc, while the corresponding fraction is only 5 % in model 6.

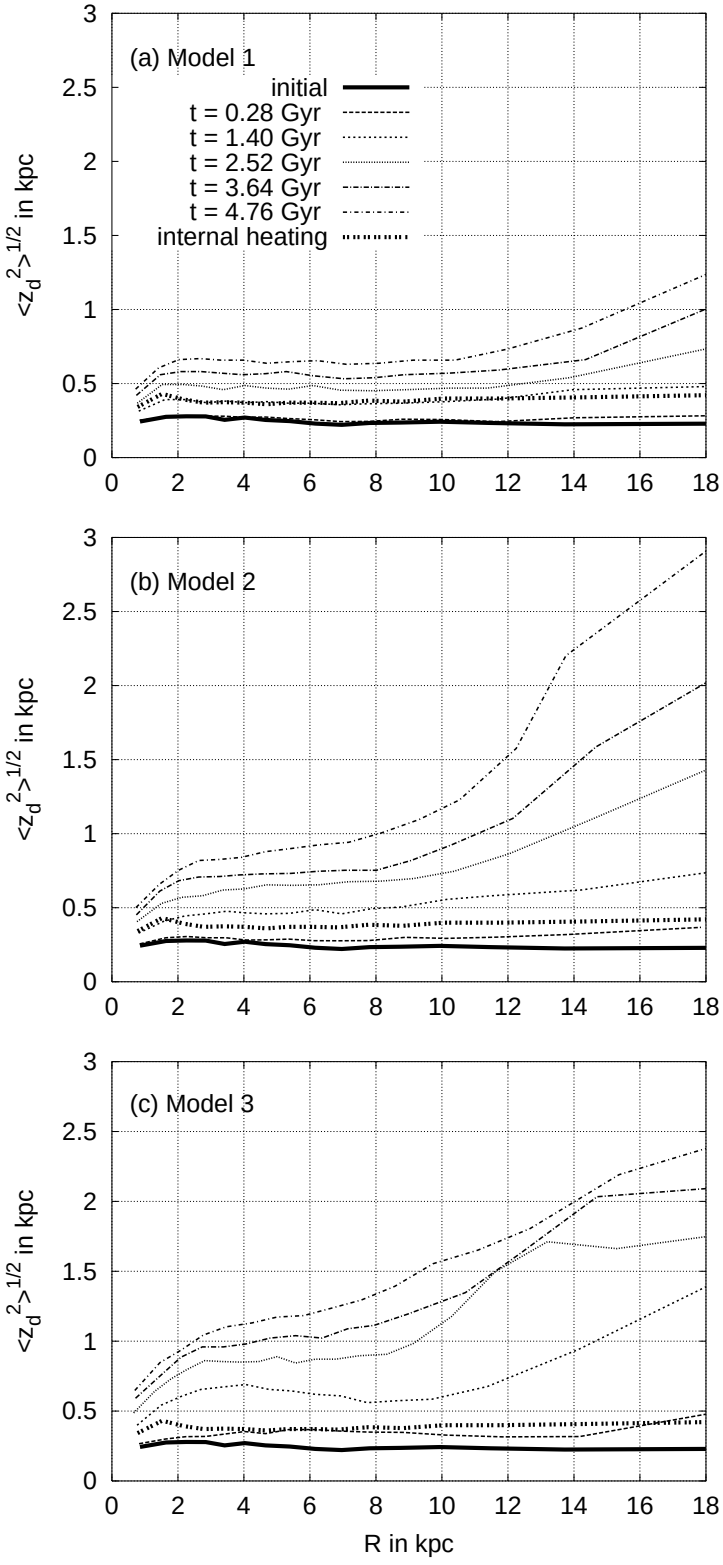


Fig. 7.— The growth of the disk vertical scale length after interaction with DM clumps with different masses given in (a) model 1 (b) model 2 (c) model 3.

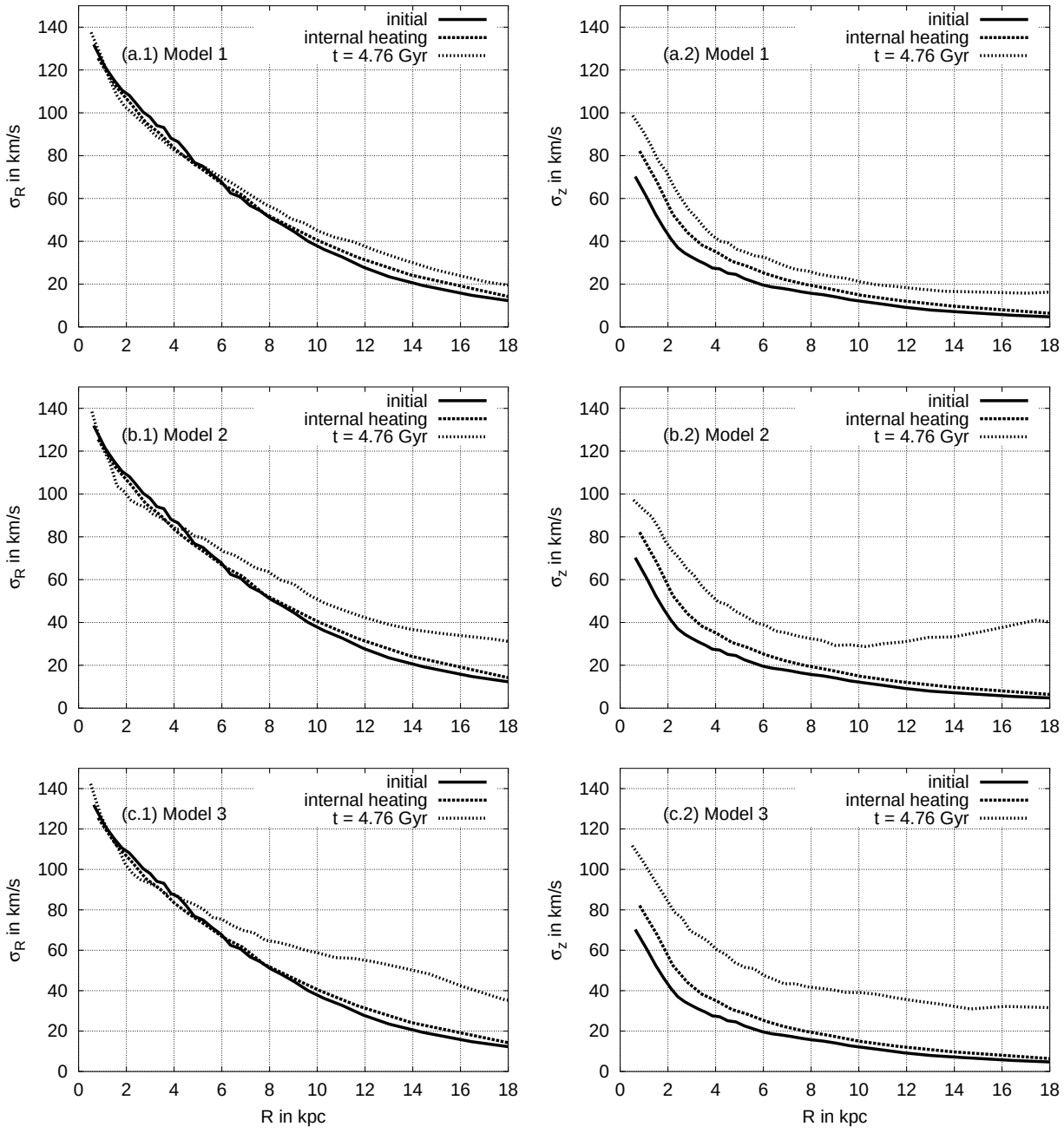


Fig. 8.— Disk velocity dispersion in vertical and radial direction after 4.76 Gyr of interaction with different mass distributions of DM clumps given in (a) model 1 (b) model 2 (c) model 3.

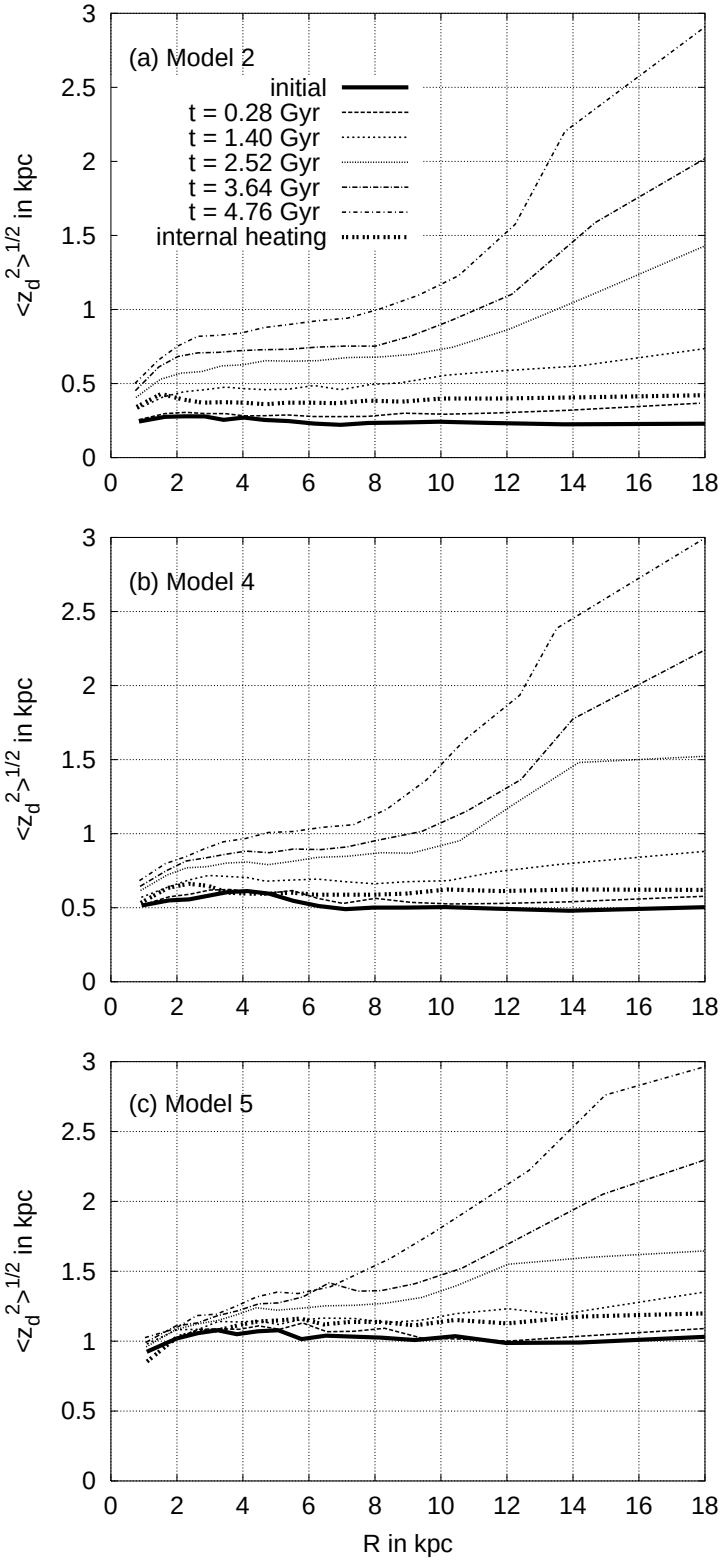


Fig. 9.— The growth of the disk vertical scale length which initially has height (a) 245 pc (b) 525 pc (c) 1050 pc, after interaction with DM clumps, specified in model 2, model 4 and model 5.

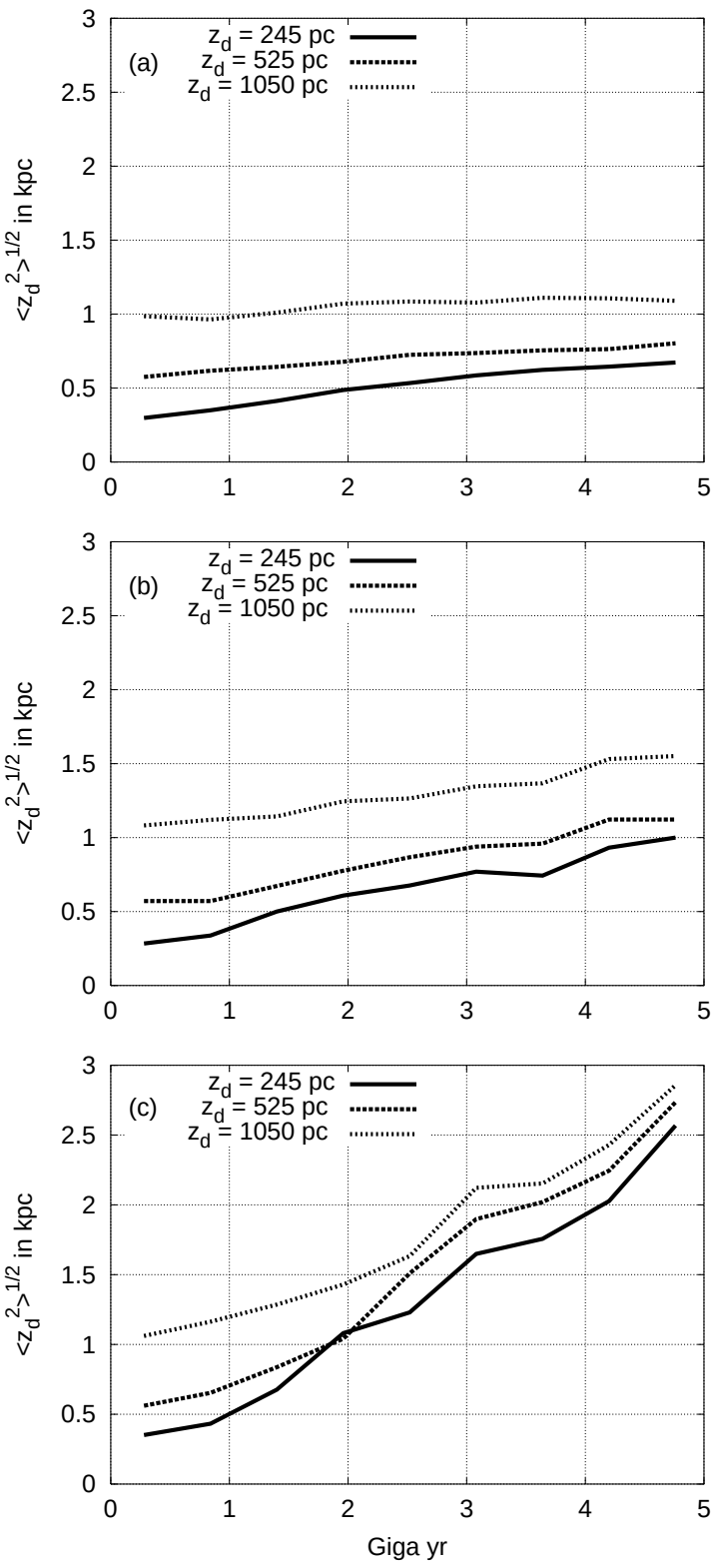


Fig. 10.— Heating of a disk with initial height 245 pc, 525 pc and 1050 pc (a) at $R = 2$ kpc, (b) at the solar radius, and (c) at $R = 16$ kpc.

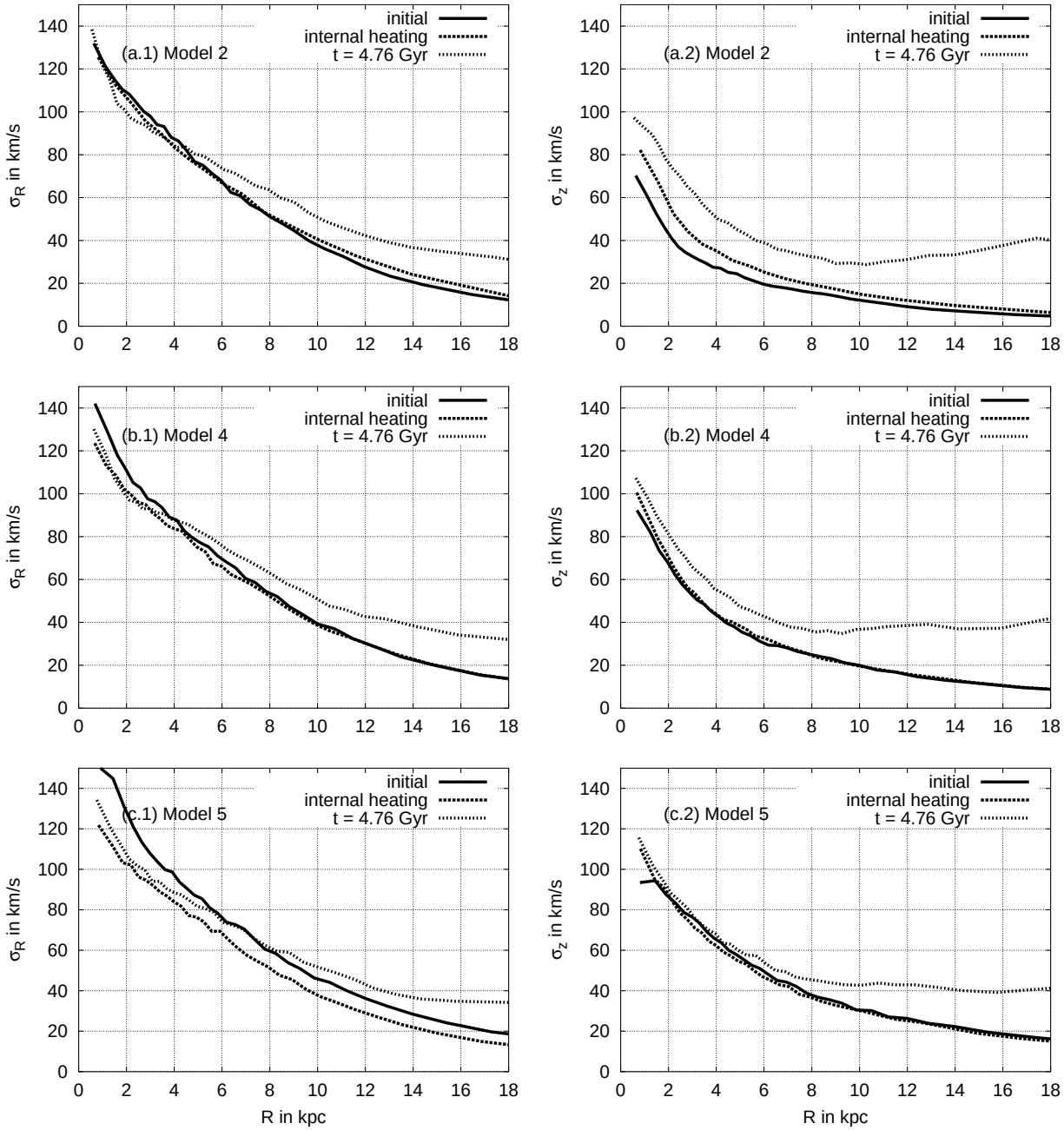


Fig. 11.— Velocity dispersion of a disk which initially has a height of (a) 245 pc (b) 525 pc (c) 1050 pc, after 4.76 Gyr of interaction with DM clumps, specified in model 2, model 4 and model 5.

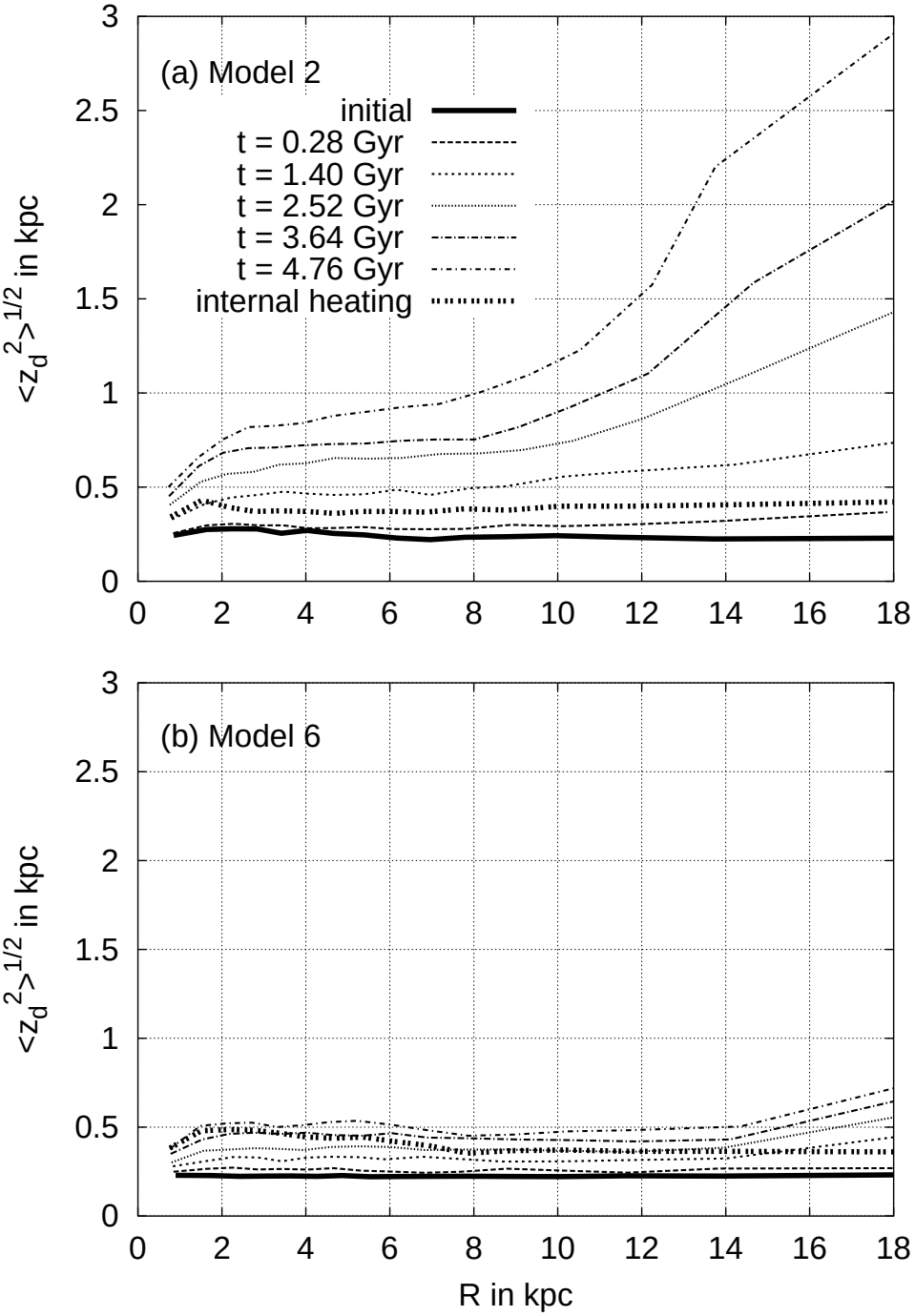


Fig. 12.— The growth of the disk vertical scale length produced by (a) model 2 where 18 % of the clumps have pericenter radii less than the solar radius and (b) model 6 with only 3.5 % of the clumps crossing the disk within the solar radius.

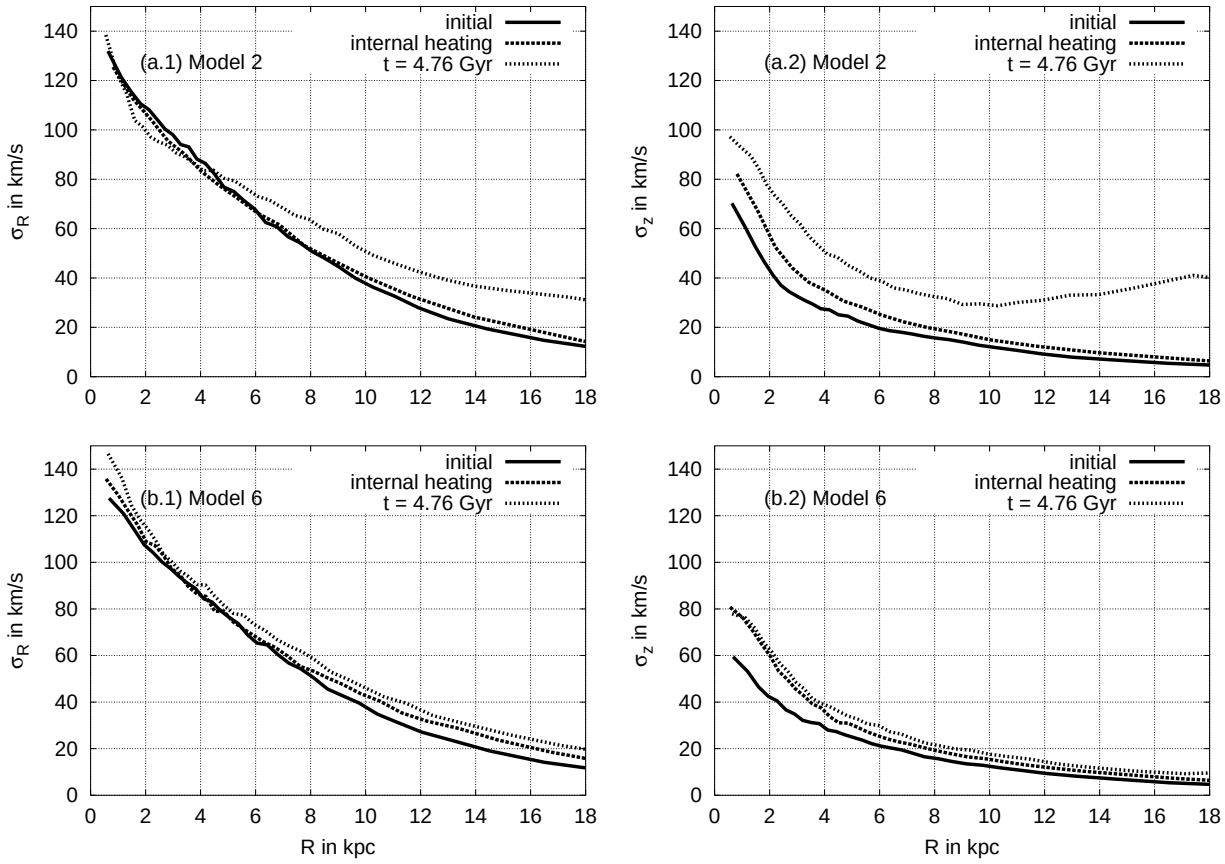


Fig. 13.— Disk velocity dispersion profiles produced by models with a fraction of clump pericenter radii inside the solar radii of (a) 18 % in model 2 and (b) 3.5 % in model 6.

Table 1. DM clumps and disk models.

| Model | Mass of each clump | Number of clumps | Disk height |
|---|---|---|---|
| Model 1 | $10^8\ M_\odot$ | 859 | 245 pc |
| Model 2 | $10^8 - 10^9\ M_\odot$ | 335 | 245 pc |
| Model 3 | $10^9\ M_\odot$ | 86 | 245 pc |
| Model 4 | $10^8 - 10^9\ M_\odot$ | 335 | 525 pc |
| Model 5 | $10^8 - 10^9\ M_\odot$ | 335 | 1050 pc |
| Model 6 | $10^8 - 10^9\ M_\odot$ | 315 | 245 pc |